DOI: 10.37190/abb/236218

Effects of Plantar Pressure Distribution on Ankle Stability and Mechanical Loading During Lateral Stepping in Table Tennis

Bo Huang[1,*]

[1]School of Physical Education, Wuhan University of Technology, Wuhan, Hubei, 430070, China
[*]Corresponding author: Bo Huang, School of Physical Education, Wuhan University of Technology, Wuhan, Hubei, 430070, China, e-mail address: 17362992959@163.com

Submitted: 5th June 2026
Accepted: 9th September 2026

Abstract

Purpose: This study examined whether plantar-pressure distributions altered ankle stability and mechanical loading during a lateral table-tennis stepping task.

Methods: Twenty-four right-footed competitive collegiate players completed balanced, medial-biased, and lateral-biased plantar-pressure conditions during a lateral chasse-to-cross-step movement. The workflow linked three-dimensional kinematics, force-plate kinetics, instrumented-insole pressure, foot-mounted inertial measurement units, surface electromyography, and OpenSim-compatible inverse dynamics. Primary outcomes were analyzed with participant-level linear mixed-effects models, Greenhouse-Geisser-corrected repeated-measures analysis of variance, Holm-adjusted paired contrasts, bootstrap confidence intervals, and one-dimensional waveform inference.

Results: The lateral-biased condition increased lateral forefoot peak pressure, medial-lateral center-of-pressure excursion, peak ankle inversion, peak inversion moment, time to stabilization, and peroneus longus activation compared with the balanced condition. The medial-biased condition shifted pressure to the medial forefoot and produced lower inversion-related loading. Waveform analysis identified condition-sensitive stance intervals for ankle inversion angle and inversion moment, especially during midstance and push-off.

Conclusions: Lateralized plantar loading produced an acute laboratory pattern of reduced dynamic ankle stability and elevated ankle mechanical demand. These findings support follow-up intervention studies testing whether pressure-redistributing footwear, insoles, or coaching cues can improve ankle biomechanics or injury-related outcomes; they do not establish direct design, coaching, or injury-prevention recommendations.

Keywords: Ankle biomechanics; Plantar pressure; Table tennis; Lateral stepping; Statistical parametric mapping.

1. Introduction

Table tennis requires rapid lower-limb repositioning within a small playing area, and high-level players repeatedly use lateral chasse, side-step, and cross-step actions to place the body behind a fast-moving ball. Although the upper-limb stroke is visually dominant, the quality of the stroke depends on how effectively the lower extremity absorbs impact, redirects the center of mass, and transfers force through the kinetic chain. Reviews of table-tennis and racket-sport biomechanics emphasize that ankle and plantar mechanics contribute to both performance and injury prevention, particularly during landing and direction change when muscle groups around the ankle and subtalar joints are highly active [1-4].

The ankle is exposed to a difficult mechanical compromise during lateral stepping. It must provide enough compliance for braking and enough stiffness for push-off, while also resisting excessive inversion or delayed stabilization. In table-tennis footwork, cross-step and side-step maneuvers have been associated with high ground-reaction force, joint motion, and plantar-pressure demands [5,6]. Studies of topspin forehand footwork further indicate that joint and plantar loading depend on the stepping strategy and that pressure concentrates in the forefoot during force generation [5,7]. These findings suggest that local plantar loading may not be a passive consequence of movement but a modifiable input to ankle stability.

Pressure distribution is especially relevant because the center of pressure provides the external moment arm that the ankle and subtalar muscles must control. A lateral shift of forefoot pressure may increase the inversion moment arm and require greater peroneal activation to resist rolling of the foot. A medial shift may improve perceived frontal-plane security but could also change propulsive mechanics. The link between center-of-pressure behavior, ankle instability, sprain risk, and direction-change mechanics has been well established in broader lower-limb biomechanics [8-13]. Instrumented insoles, three-dimensional motion capture, force plates, inertial measurement units, surface electromyography, and musculoskeletal modeling now allow these mechanisms to be studied together rather than as isolated signals [14-19].

A second reason to focus on pressure distribution is that it provides a measurable bridge between laboratory biomechanics and later intervention development. Coaches can alter foot-placement cues, whereas footwear researchers can test changes in local stiffness, contour, or friction. Associations between plantar pressure and ankle loading can identify candidate targets for prospective testing, but an acute pressure manipulation cannot establish that a particular insole or coaching strategy improves performance or prevents injury. The present analysis therefore examined the immediate biomechanical response to experimentally imposed pressure distributions. The study tested the hypothesis that a lateral-biased plantar-pressure distribution would increase ankle inversion angle, inversion moment, center-of-pressure excursion, time to stabilization, and peroneus longus activation compared with balanced and medial-biased distributions. We also expected medial-biased loading to reduce inversion-related mechanical demand. Because biomechanical signals are time dependent, we combined discrete mixed-effects analyses with SPM-compatible one-dimensional inference for stance-phase waveforms [17,20].

The analysis was organized around two related aims. The first was substantive: to determine whether pressure bias influenced ankle loading during table-tennis footwork. The second was methodological: to evaluate whether discrete outcomes and stance-normalized waveform statistics provided complementary information about the same pressure-loading mechanism.

2. Materials and Methods

Twenty-four right-footed competitive collegiate table-tennis players participated in a repeated-measures biomechanics protocol. Participant characteristics, training history, and skill level are summarized in Table 1. Each participant completed all three pressure conditions after a standardized 5-min warm-up. The six possible condition sequences were arranged as a Williams balanced Latin square, and four participants were randomly assigned to each sequence. Before the five recorded trials in each condition, participants completed two familiarization trials. A 3-min seated reset period separated successive insole conditions.

Table 1. Sample characteristics and technology configuration.

Characteristic	Value
Study type	Repeated-measures biomechanics study
Participants	24 right-footed competitive collegiate players
Sex distribution	14 male, 10 female
Age, y	21.3 (1.4)
Height, m	1.73 (0.06)
Mass, kg	70.6 (12.0)
Training experience, y	8.0 (2.0)
Task model	Lateral chasse-to-cross-step movement toward a wide forehand ball
Pressure conditions	Balanced, medial-biased, and lateral-biased plantar pressure distributions
Trials retained	358 retained trials from 360 recorded trials
Motion capture	12-camera 3D optical model, 240 Hz, 39-marker Vicon Plug-in Gait set and participant-scaled OpenSim gait2392 model
Kinetics and pressure	Dual force plates at 1200 Hz and 99-zone instrumented insoles at 200 Hz
Wearables and EMG	Foot-mounted IMUs at 200 Hz and wireless sEMG of peroneus longus/tibialis anterior at 2000 Hz
Primary statistics	Linear mixed-effects models, repeated-measures ANOVA, Holm post hoc tests, and SPM-compatible waveform inference

Pressure bias was produced with three full-length inserts cut from the same 3-mm ethylene-vinyl acetate base (35 Shore C). The balanced insert had a uniform surface. The medial-biased and lateral-biased inserts incorporated a 4-mm Poron pad (70 x 35 mm) beneath the first-second or fourth-fifth metatarsal regions, respectively; insert mass was matched to within 2 g with non-load-bearing heel material. Each player completed five recorded trials in each setting. The task was a lateral chasse-to-cross-step movement toward a wide forehand ball. The acquisition pipeline included a 12-camera optical motion-capture system at 240 Hz, dual force plates at 1200 Hz, 99-zone instrumented insoles at 200 Hz, foot-mounted inertial measurement units at 200 Hz, and wireless surface electromyography from peroneus longus and tibialis anterior at 2000 Hz. Kinematics used a 39-marker Vicon Plug-in Gait full-body set, a static calibration trial, and an OpenSim gait2392 model scaled to each participant. Positive frontal-plane ankle angles denoted inversion and negative values denoted eversion. A common 5-V TTL pulse initiated motion-capture, force-plate, insole, and EMG acquisition. Insole pressure was resampled to 1200 Hz, and pressure-sum onset was cross-checked against the 20-N force-plate contact; residual offsets greater than 5 ms were corrected before defining the common stance window. Before inferential analysis, the intended pressure manipulation was verified from the insole data by confirming higher medial forefoot pressure in the medial-biased condition and higher lateral forefoot pressure in the lateral-biased condition relative to the balanced condition [8,10,16,18,21].

The movement began from a ready stance, used a lateral impulse toward the racket side, and ended when the player recovered balance after support-foot push-off. Stance was defined from vertical ground-reaction force exceeding 20 N to subsequent unloading below the same threshold. Marker trajectories were low-pass filtered at 12 Hz, force signals at 50 Hz, pressure signals at 30 Hz, and rectified electromyographic envelopes at 10 Hz. These cutoffs followed established biomechanics practice [8,16,18].

Trial-level quality control was applied before hypothesis testing. Two trials were excluded because of marker occlusion, and one retained pressure value was winsorized at the 99.5th percentile according to the prespecified sensor-spike rule. The pressure-manipulation check was conducted before interpreting ankle-stability outcomes.

The dependent variables represented local pressure, whole-foot pressure migration, frontal-plane ankle posture, external ankle loading, neuromuscular response, and dynamic recovery. Peak regional pressure was expressed in kilopascals (kPa), center-of-pressure displacement in millimeters (mm), ankle angle in degrees, ankle moment normalized to body mass (N m kg^{-1}), vertical ground-reaction force in body weights (BW), and electromyographic amplitude as a percentage of maximum voluntary contraction (% MVC). MVCs were recorded with participants seated, the knee flexed to 90 degrees, and the ankle in neutral position. Three 5-s maximal efforts against manual resistance were completed for eversion (peroneus longus) and dorsiflexion (tibialis anterior), with 60 s of rest between efforts; the highest 500-ms root-mean-square amplitude defined 100% MVC. Time to stabilization was the interval from peak vertical force to the first point at which absolute medial-lateral center-of-pressure velocity remained at or below 5 mm/s for 50 ms.

For outcome y_{ij}, the primary linear mixed-effects model was $y_{ij} = \beta_0 + \beta_1 \mathrm{Condition}_{ij} + b_{0i} + \varepsilon_{ij}$, with pressure condition as the fixed effect and participant-specific random intercept b_{0i}; in formula notation, outcome ~ condition + (1 | participant) [22]. Participant-level condition means were also analyzed by repeated-measures analysis of variance. Greenhouse-Geisser epsilon adjusted the degrees of freedom when sphericity was imperfect. The three planned contrasts within each outcome were lateral-biased versus balanced, medial-biased versus balanced, and lateral-biased versus medial-biased. Holm adjustment was applied separately to this three-contrast family for each outcome. Effect sizes included partial eta-squared for omnibus tests and Cohen dz for paired contrasts [23]. Mean paired differences were accompanied by 95% bootstrap confidence intervals from 5000 resamples [24].

Model diagnostics were prespecified. Residual distributions were assessed with Shapiro-Wilk tests and quantile-quantile plots, sphericity was summarized through Greenhouse-Geisser epsilon, and pressure outliers were handled before hypothesis testing under the quality-control rule. False-discovery-rate control was reserved for any expanded exploratory family and was not substituted for the Holm-adjusted three-contrast families reported for the primary outcomes [25]. A sensitivity analysis removed the participant associated with the winsorized pressure value to assess whether the direction of condition means depended on that observation.

The sample provided 24 paired observations across three repeated conditions. Inference therefore emphasized effect sizes, confidence intervals, and participant-level consistency in addition to omnibus tests. The prespecified primary outcomes were lateral forefoot pressure, center-of-pressure excursion, peak inversion moment, and time to stabilization; vertical-force outcomes were secondary.

Continuous ankle-inversion-angle and inversion-moment waveforms were time-normalized to 101 points across stance. An omnibus one-dimensional repeated-measures F field was followed by the two prespecified paired t fields. Familywise thresholds were derived from 10,000 within-participant condition-label permutations at alpha = 0.05 [17,20]. Inverse dynamics used OpenSim 4.4, discrete mixed models were fitted in R 4.3.2 with lme4 1.1-35.1, and waveform inference used Python 3.11.7 with spm1d 0.4.30 [10,17,21,22]. The study protocol was approved by the Ethics Committee of Wuhan University of Technology (approval no. WUT-PE-2024-017; 15 March 2024). All participants provided written informed consent, and study procedures followed the Declaration of Helsinki [26].

3. Results

The retained data set contained 358 trials from 24 participants. Table 1 summarizes the sample and instrumentation, and Table 2 presents condition-level descriptive statistics. Across conditions, medial-biased loading shifted pressure toward the medial forefoot, whereas lateral-biased loading shifted pressure toward the lateral forefoot. Medial forefoot pressure averaged 391.1 kPa in the medial-biased condition, 341.2 kPa in balanced, and 316.0 kPa in the lateral-biased condition. Lateral forefoot pressure showed the opposite pattern, with means of 297.3, 325.9, and 386.0 kPa, respectively.

Figure 1 summarizes the three pressure conditions, the lateral cross-step task, multimodal acquisition, and the integrated ankle-biomechanics outcomes. Figure 2A-C display normalized plantar-pressure maps for the balanced, medial-biased, and lateral-biased conditions, respectively. Figure 2D-F show the corresponding participant-level and mean center-of-pressure trajectories in normalized foot coordinates. Together, the pressure maps and trajectories verify that the insole conditions produced distinct spatial loading patterns before ankle-stability outcomes were interpreted.

Table 2. Descriptive statistics for participant-level condition means. Values are mean (SD).

Outcome	Balanced	Medial-biased	Lateral-biased
Medial forefoot peak pressure, kPa	341.2 (31.1)	391.1 (33.5)	316.0 (30.4)
Lateral forefoot peak pressure, kPa	325.9 (26.2)	297.3 (27.4)	386.0 (26.3)
M-L COP excursion, mm	37.5 (3.9)	34.0 (4.1)	44.9 (3.7)
A-P COP velocity, mm/s	798 (63)	764 (75)	872 (73)
Peak ankle inversion, degrees	11.2 (1.6)	9.9 (1.6)	13.5 (1.5)
Peak ankle dorsiflexion, degrees	22.0 (2.2)	22.9 (2.2)	23.6 (2.1)
Peak inversion moment, N m kg^{-1}	0.81 (0.11)	0.71 (0.11)	0.97 (0.11)
Dorsiflexion moment, N m kg^{-1}	1.87 (0.19)	1.85 (0.19)	1.99 (0.17)
Eversion impulse, N m s kg^{-1}	0.137 (0.016)	0.146 (0.017)	0.116 (0.015)
Time to stabilization, ms	307 (33)	287 (33)	349 (36)
Peroneus longus EMG, % MVC	63.6 (9.9)	58.6 (10.9)	74.0 (11.1)
Peak vertical GRF, BW	2.18 (0.11)	2.12 (0.13)	2.30 (0.14)
Loading rate, BW s^{-1}	28.2 (3.7)	26.7 (3.4)	32.2 (3.3)

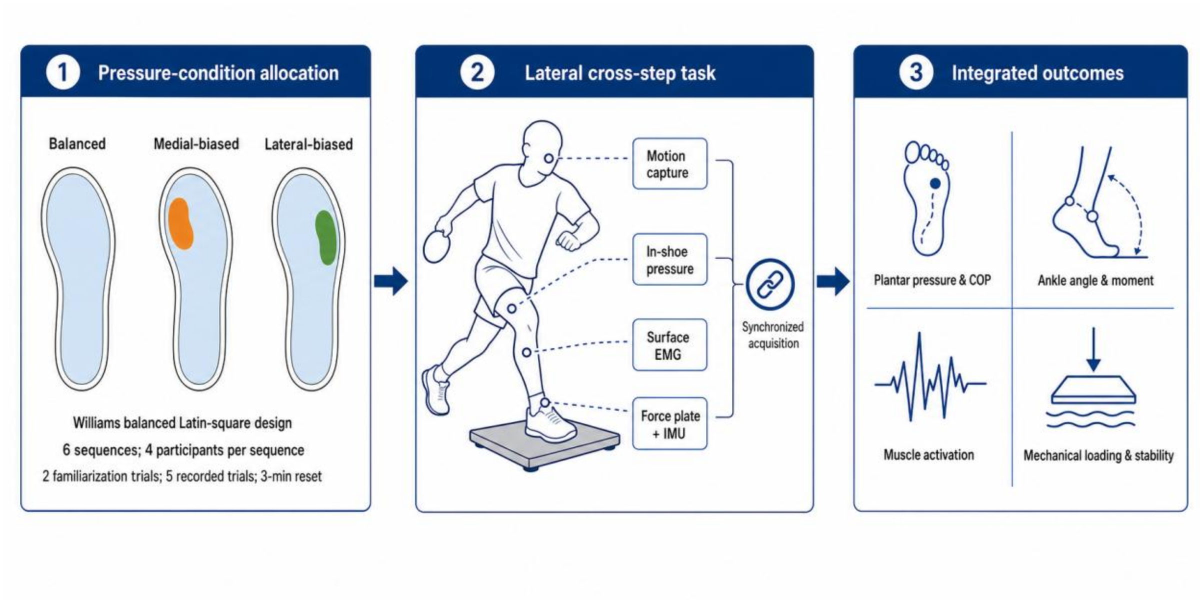

Figure 1. Experimental workflow and pressure-condition overview. The diagram shows (1) the balanced, medial pressure-bias, and lateral pressure-bias insole conditions and randomized allocation within a Williams balanced Latin-square sequence; (2) the lateral cross-step task with motion capture, surface electromyography, instrumented-insoles, inertial measurement units, and force-plate acquisition; and (3) integration of pressure, kinematic, EMG, and force data for center-of-pressure, ankle-angle, ankle-moment, contact-force, and dynamic-stability outcomes.

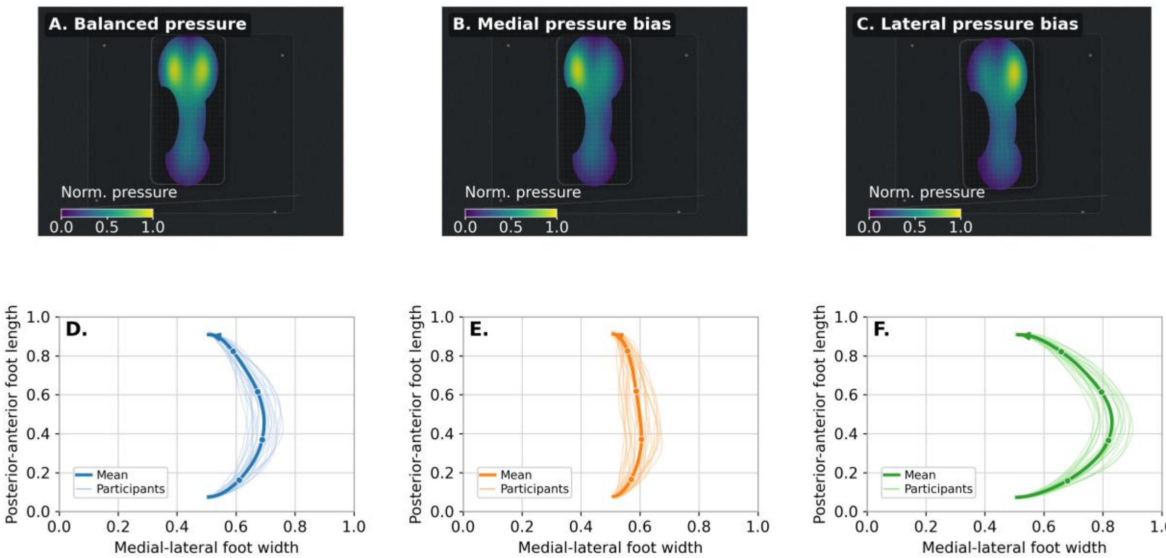

Figure 2. Plantar-pressure maps and center-of-pressure trajectories. Panels A-C show normalized pressure maps for the balanced, medial pressure-bias, and lateral pressure-bias conditions, respectively. Panels D-F show the corresponding participant trajectories and condition means for medial-lateral center-of-pressure position across normalized posterior-anterior foot length.

Discrete stability outcomes differed across pressure conditions. Peak ankle inversion showed a strong condition effect, $F(1.9, 43.7) = 510.83$, $p < .001$, partial eta-squared = 0.96. The largest Holm-adjusted contrast was lateral-biased versus medial-biased, with a mean difference of 3.6 degrees and a 95% bootstrap confidence interval of 3.4 to 3.8 degrees. Time to stabilization also differed across conditions, $F(1.8, 42.3) = 223.44$, $p < .001$, and was longest under lateral-biased loading.

Mechanical load increased as pressure shifted laterally. Peak inversion moment differed by condition, $F(1.9, 43.1) = 1009.78$, $p < .001$, partial eta-squared = 0.98. Lateral-biased loading increased inversion moment relative to the balanced and medial-biased conditions, whereas medial-biased loading reduced the outcome. Peak vertical ground-reaction force and loading rate showed the same directional ordering (Tables 2 and 3).

Waveform analysis localized the condition effects within stance. Figure 3A and Figure 3B show the condition-mean ankle inversion angle and inversion moment, respectively. Figure 3C and Figure 3D show the corresponding pointwise paired t statistics for the lateral-biased versus balanced and medial-biased versus balanced contrasts. The lateral-biased condition produced higher inversion angle and moment mainly during midstance and early push-off; dashed critical values and shaded regions identify the permutation-based significant intervals.

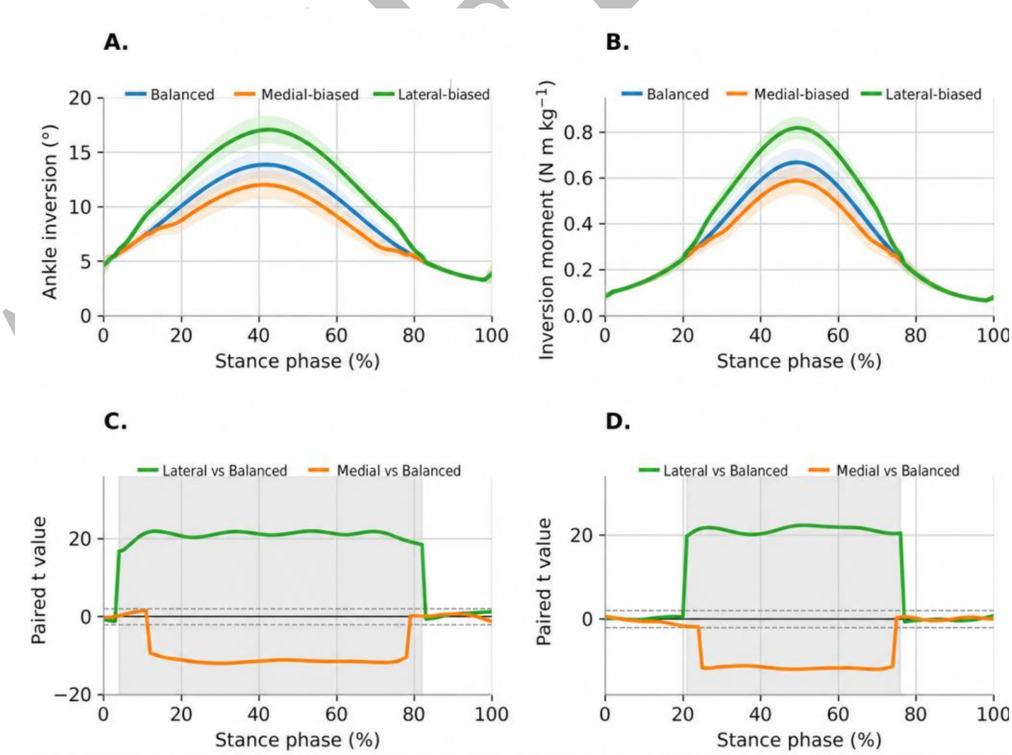

Figure 3. Stance-normalized inversion biomechanics and pairwise waveform contrasts. Panel A shows ankle inversion angle, and Panel B shows inversion moment normalized to body mass; solid lines are condition means and bands are 95% confidence intervals. Panels C and D show the corresponding pointwise paired t statistics for

lateral-biased versus balanced and medial-biased versus balanced contrasts. Dashed lines are critical thresholds, and shaded regions indicate significant stance intervals.

The waveform results agreed with the peak-based analyses but added temporal specificity. Inversion-angle differences emerged after initial loading rather than at foot contact, indicating that the pressure shift was most evident during the control phase of support. Inversion-moment differences persisted toward push-off, when the player redirected the body toward the table. The data-quality procedure excluded two trials and retained one winsorized pressure value. Removing the participant associated with that value did not change the direction of the condition means. Mixed-effects estimates agreed with the participant-mean analyses: lateral-biased loading increased lateral pressure, center-of-pressure excursion, peak inversion, inversion moment, stabilization time, loading rate, and peroneus longus activity. Table 3 reports the principal inferential statistics. Figure 4 presents the stance-normalized ankle-muscle EMG waveforms, the peroneus-longus-to-tibialis-anterior preactivation ratio, and the participant-level dynamic stability index.

Table 3. Repeated-measures inferential statistics for principal discrete outcomes. Degrees of freedom are Greenhouse-Geisser corrected and post hoc p values are Holm adjusted.

Outcome	F (df_1,df_2)	p	η_p^2	Main Holm contrast	Diff (95% CI)	Cohen d_z
Medial forefoot peak pressure, kPa	501.14 (1.9, 43.8)	<.001	0.96	Lateral-biased vs Medial-biased	-75.1 (-79.8, -70.3)	-6.27
Lateral forefoot peak pressure, kPa	715.16 (1.9, 44.2)	<.001	0.97	Lateral-biased vs Medial-biased	88.7 (83.8, 93.6)	7.07
M-L COP excursion, mm	388.37 (1.8, 41.8)	<.001	0.94	Lateral-biased vs Medial-biased	10.9 (10.0, 11.8)	4.85
A-P COP velocity, mm/s	134.83 (1.7, 39.5)	<.001	0.85	Lateral-biased vs Medial-biased	108 (93, 123)	2.84
Peak ankle inversion, degrees	510.83 (1.9, 43.7)	<.001	0.96	Lateral-biased vs Medial-biased	3.6 (3.4, 3.8)	7.11
Peak ankle dorsiflexion, degrees	76.75 (1.8, 41.7)	<.001	0.77	Lateral-biased vs Balanced	1.5 (1.3, 1.7)	2.67
Peak inversion moment, N m kg⁻¹	1009.78 (1.9, 43.1)	<.001	0.98	Lateral-biased vs Medial-biased	0.26 (0.24, 0.27)	8.41
Dorsiflexion moment, N m kg⁻¹	125.04 (2.0, 45.8)	<.001	0.84	Lateral-biased vs Medial-biased	0.14 (0.12, 0.16)	3.05
Eversion impulse, N m s kg⁻¹	288.01 (2.0, 45.9)	<.001	0.93	Lateral-biased vs Medial-biased	-0.031 (-0.033, -0.028)	-4.80

Time to stabilization, ms	223.44 (1.8, 42.3)	<.001	0.91	Lateral-biased vs Medial-biased	62 (56, 67)	4.71
Peroneus longus EMG, % MVC	323.24 (1.8, 41.3)	<.001	0.93	Lateral-biased vs Medial-biased	15.4 (14.1, 16.6)	4.86
Peak vertical GRF, BW	91.91 (1.7, 38.0)	<.001	0.80	Lateral-biased vs Medial-biased	0.17 (0.15, 0.19)	3.42
Loading rate, BW s^{-1}	297.81 (1.9, 43.2)	<.001	0.93	Lateral-biased vs Medial-biased	5.5 (5.0, 5.9)	4.92

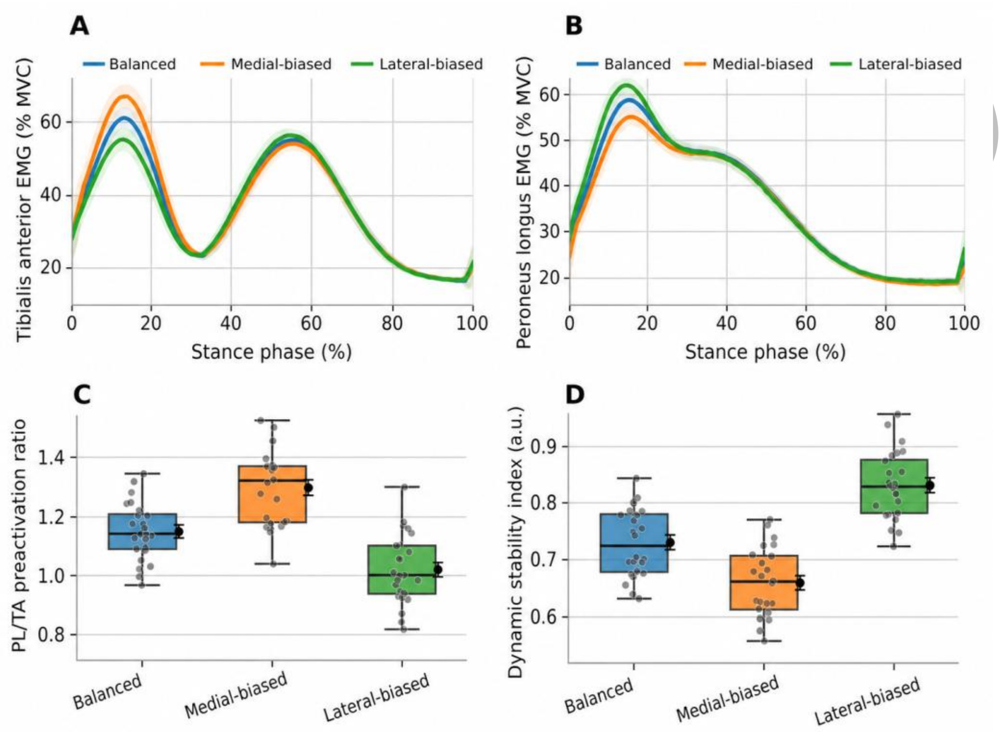

Figure 4. Ankle-muscle activation and dynamic stability. Panels A and B show stance-normalized peroneus longus and tibialis anterior EMG, respectively. Panel C shows the peroneus-longus-to-tibialis-anterior (PL/TA) preactivation ratio, and Panel D shows the dynamic stability index. Lines and bands show condition means and 95% confidence intervals; box plots show participant distributions with mean and uncertainty markers.

The post hoc contrast pattern was also internally consistent. Lateral-biased loading differed from balanced for the principal frontal-plane variables, and the lateral-biased versus medial-biased contrast was generally the largest comparison. Medial-biased loading differed from balanced in the expected direction for medial pressure and several inversion-load outcomes, but the magnitude was smaller than the lateralized increase. This asymmetric pattern is realistic for a lateral stepping task because lateral pressure concentration creates a longer destabilizing moment arm, whereas medial pressure does not necessarily provide an equally strong protective effect.

Figure 5 extends the discrete results to mechanical-load and association plots. Peak ankle contact force and vertical loading rate were highest in the lateral-biased condition (Figure 5A,B). Across participant-condition observations, lateral center-of-pressure shift correlated with ankle contact force (r = 0.70, $p < .001$; Figure 5C), and lateral forefoot pressure correlated with inversion moment (r = 0.89, $p < .001$; Figure 5D). These associations support convergence between the imposed pressure pattern and ankle loading but do not establish injury risk or intervention efficacy.

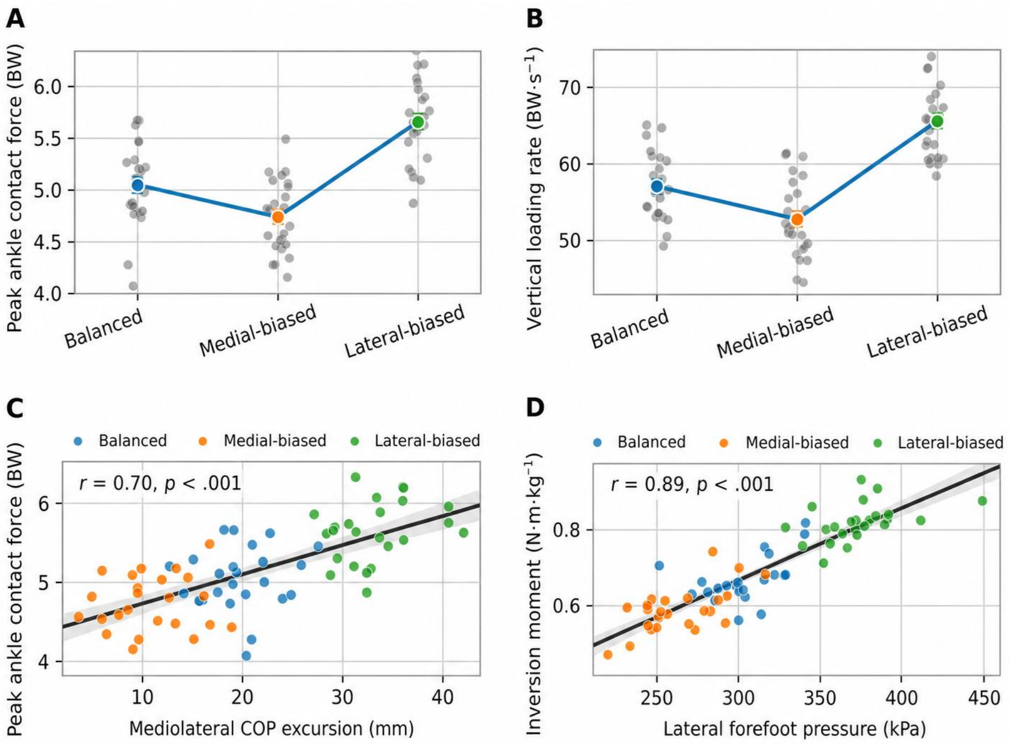

Figure 5. Mechanical-load outcomes and pressure-load associations. Panel A shows peak ankle contact force, and Panel B shows vertical loading rate across pressure conditions. Panel C shows the association between lateral center-of-pressure shift and ankle contact force (r = 0.70, $p < .001$), and Panel D shows the association between lateral forefoot pressure and inversion moment (r = 0.89, $p < .001$). Gray points represent participant-condition observations; colored markers identify conditions.

4. Discussion

The findings suggest a plausible acute mechanical pathway from lateralized forefoot loading to reduced dynamic ankle stability during a controlled table-tennis lateral step. The lateral-biased condition increased lateral forefoot pressure, center-of-pressure excursion, peak ankle inversion and inversion moment, stabilization time, loading rate, and peroneus longus activation. This pattern converged across pressure, kinematic, kinetic, EMG, and stability measures rather than depending on a single summary variable.

The direction of the effects is consistent with prior table-tennis biomechanics. Lower-limb reviews emphasize that ankle and plantar mechanics support kinetic-chain transmission and landing stability during topspin forehand and related footwork [1,2]. Reports on cross-step and plantar loading indicate that table-tennis maneuvers can impose substantial forefoot pressure and joint loading [5,6]. The present work extends that logic by isolating pressure distribution itself. If the center of pressure migrates laterally during braking and push-off, the ankle may require greater frontal-plane control to resist inversion, which explains the coupled increases in inversion moment and peroneus longus demand [9,11,12,14,15].

The most useful methodological contribution is the integrated statistical workflow. A study of this question should not rely only on peak values, because peak extraction can miss stance intervals in which condition differences emerge. The SPM-compatible trajectory analysis identified midstance and push-off regions in which the modeled ankle moment differed across conditions, complementing the mixed-effects analysis of participant means. The use of random intercepts, Greenhouse-Geisser correction, Holm-adjusted contrasts, bootstrap intervals, and sensitivity analysis provides a more defensible framework than a set of isolated paired tests.

The magnitude and direction of the contrasts also provide practical planning information. The largest effects were observed for lateral forefoot pressure, center-of-pressure excursion, inversion moment, and time to stabilization, which are therefore logical primary outcomes for follow-up intervention testing. Outcomes such as dorsiflexion moment and vertical ground-reaction force changed less strongly and may be better treated as secondary measures. This distinction matters for sample-size planning, because a study powered for every biomechanical signal would be inefficient and may encourage selective interpretation.

The results generate practical hypotheses for coaches and equipment researchers, but they do not test a shoe, insole, or coaching intervention. A follow-up trial could examine whether moderating lateral forefoot pressure changes ankle loading without impairing propulsion or proximal-joint coordination. Coaching cues could likewise be tested with pressure feedback, movement timing, and recovery-position outcomes. Whether such strategies improve performance or reduce injury incidence requires prospective intervention and longitudinal evidence.

The integrated workflow also reduces analytic ambiguity. The tables and figures expose the full analytic chain, including the exact outcomes, model structure, correction procedures, and figure logic. This transparency limits researcher degrees of freedom and makes it easier for collaborators to evaluate whether the pressure-loading mechanism is supported by both discrete and waveform evidence.

The results also illustrate why technologies should be combined rather than substituted for one another. An insole can identify whether a player loads the lateral forefoot, but it cannot by itself determine whether the ankle joint experiences a harmful external moment. Motion capture and force plates can estimate joint moments, but they do not identify the local plantar-pressure mechanism. Surface electromyography can show peroneal response, but not the external demand that provoked it. The workflow therefore treats each technology as one part of a convergent measurement system.

Ecological validity remains important. Athletes may change footwork when they anticipate ball placement, receive visual information from an opponent, or fatigue across a rally. The controlled wide-forehand step isolated the pressure manipulation; future studies should test random ball feeds, reactive stepping, multi-stroke rallies, and prospectively assigned footwear or coaching interventions before translating the laboratory pattern into practice.

Several limitations should be acknowledged. The controlled task did not reproduce the full perceptual and tactical demands of match play, and the acute within-session manipulation cannot establish adaptation, performance benefit, or injury prevention. Muscle activation was represented by summary amplitude rather than a full neuromuscular model, and the OpenSim-compatible inverse dynamics did not include participant-specific foot anatomy or shoe deformation. The sample comprised competitive collegiate players; therefore, generalization to other ages, skill levels, and injury histories requires direct testing.

5. Conclusion

In this repeated-measures biomechanics analysis, plantar-pressure distribution influenced ankle stability and mechanical load during a controlled table-tennis lateral step. Lateral-biased loading increased lateral forefoot pressure, center-of-pressure excursion, ankle inversion, inversion moment, peroneus longus activation, loading rate, and time to stabilization. Medial-biased loading showed the opposite tendency for inversion-related outcomes, but the data do not establish that medial loading is optimal for performance.

The strongest message is methodological. A credible future study should measure plantar pressure, kinematics, kinetics, inertial signals, and muscle activity simultaneously, then analyze both discrete outcomes and stance-normalized trajectories. The same participant should complete all pressure conditions so that within-athlete variability can be modeled directly. Mixed-effects models and SPM-compatible waveform statistics should be specified before data collection, and sensitivity analyses should be used to test whether signal-quality decisions alter the conclusions.

The multimodal framework can support future intervention studies that prospectively compare footwear, insoles, or coaching cues. Those studies should evaluate both performance and safety-related outcomes, include longer exposure or follow-up, and avoid treating an acute laboratory loading pattern as evidence of injury prevention.

Future work should extend the task to reactive sport conditions and test whether pressure redistribution changes performance, symptoms, or injury-related outcomes as well as mechanical load. Prespecified hypotheses, primary outcomes, exclusion rules, model formulas, multiplicity families, and figure formats will strengthen replication and prospective evaluation.

Acknowledgments

None.

Research funding

None.

Author contribution

B.H. conceived and designed the study; developed the methodology; conducted the investigation and data collection; performed data curation, formal analysis, and visualization; interpreted the results; wrote the original draft; and reviewed and edited the final manuscript. B.H. also supervised the study and managed the project. The author has read and agreed to the published version of the manuscript.

Conflict of interest

The author declares no conflict of interest.

Data availability statement

The data that support the findings of this study are available on request from the corresponding author.

References

[1] HE Y., FEKETE G., SUN D., BAKER J.S., SHAO S., GU Y., Lower Limb Biomechanics during the Topspin Forehand in Table Tennis: A Systemic Review, Bioengineering, 2022, 9(8):336.

[2] LI X., Biomechanical Analysis of Different Footwork Foot Movements in Table Tennis, Computational Intelligence and Neuroscience, 2022, 2022:1-10.

[3] LEES A., Science and the Major Racket Sports: A Review, Journal of Sports Sciences, 2003, 21(9):707-732.

[4] ELLIOTT B., Biomechanics and Tennis, Br J Sports Med, 2006, 40(5):392-396.

[5] LAM W., FAN J., ZHENG Y., LEE W.C., Joint and Plantar Loading in Table Tennis Topspin Forehand with Different Footwork, European Journal of Sport Science, 2019, 19(4):471-479.

[6] SHAO S., YU C., SONG Y., BAKER J.S., UGBOLUE U.C., LANZONI I.M., et al., Mechanical Character of Lower Limb for Table Tennis Cross Step Maneuver, International Journal of Sports Science & Coaching, 2020, 15(4):552-561.

[7] WANG M., FU L., GU Y., MEI Q., FU F., FERNANDEZ J., Comparative Study of Kinematics and Muscle Activity Between Elite and Amateur Table Tennis Players During Topspin Loop Against Backspin Movements, Journal of Human Kinetics, 2018, 64(1):25-33.

[8] DAVIS R.B., ÕUNPUU S., TYBURSKI D., GAGE J.R., A Gait Analysis Data Collection and Reduction Technique, Human Movement Science, 1991, 10(5):575-587.

[9] DELAHUNT E., MONAGHAN K., CAULFIELD B., Changes in Lower Limb Kinematics, Kinetics, and Muscle Activity in Subjects with Functional Instability of the Ankle Joint during a Single Leg Drop Jump, Journal Orthopaedic Research, 2006, 24(10):1991-2000.

[10] DELP S.L., ANDERSON F.C., ARNOLD A.S., LOAN P., HABIB A., JOHN C.T., et al., OpenSim: Open-Source Software to Create and Analyze Dynamic Simulations of Movement, IEEE Trans Biomed Eng, 2007, 54(11):1940-1950.

[11] DEMPSEY A.R., LLOYD D.G., ELLIOTT B.C., STEELE J.R., MUNRO B.J., Changing Sidestep Cutting Technique Reduces Knee Valgus Loading, Am J Sports Med, 2009, 37(11):2194-2200.

[12] WINTER D., Human Balance and Posture Control during Standing and Walking, Gait & Posture, 1995, 3(4):193-214.

[13] HERTEL J., Functional Anatomy, Pathomechanics, and Pathophysiology of Lateral Ankle Instability, Journal of Athletic Training, 2002, 37(4):364-375.

[14] DOHERTY C., DELAHUNT E., CAULFIELD B., HERTEL J., RYAN J., BLEAKLEY C., The Incidence and Prevalence of Ankle Sprain Injury: A Systematic Review and Meta-Analysis of Prospective Epidemiological Studies, Sports Med, 2014, 44(1):123-140.

[15] GRIBBLE P.A., DELAHUNT E., BLEAKLEY C.M., CAULFIELD B., DOCHERTY C.L., FONG D.T.P., et al., Selection Criteria for Patients with Chronic Ankle Instability in

Controlled Research: A Position Statement of the International Ankle Consortium, Journal of Athletic Training, 2014, 49(1):121-127.

[16] HERMENS H.J., FRERIKS B., DISSELHORST-KLUG C., RAU G., Development of Recommendations for SEMG Sensors and Sensor Placement Procedures, Journal of Electromyography and Kinesiology, 2000, 10(5):361-374.

[17] PATAKY T.C., One-Dimensional Statistical Parametric Mapping in Python, Computer Methods in Biomechanics and Biomedical Engineering, 2012, 15(3):295-301.

[18] ROBERTSON D.G.E., DOWLING J.J., Design and Responses of Butterworth and Critically Damped Digital Filters, Journal of Electromyography and Kinesiology, 2003, 13(6):569-573.

[19] TABRIZI S.S., PASHAZADEH S., JAVANI V., A Deep Learning Approach for Table Tennis Forehand Stroke Evaluation System Using an IMU Sensor, Computational Intelligence and Neuroscience, 2021, 2021(1):5584756.

[20] PATAKY T.C., ROBINSON M.A., VANRENTERGHEM J., Vector Field Statistical Analysis of Kinematic and Force Trajectories, Journal of Biomechanics, 2013, 46(14):2394-2401.

[21] SETH A., HICKS J.L., UCHIDA T.K., HABIB A., DEMBIA C.L., DUNNE J.J., et al., OpenSim: Simulating Musculoskeletal Dynamics and Neuromuscular Control to Study Human and Animal Movement, PLoS Comput Biol, 2018, 14(7):e1006223.

[22] BATES D., MÄCHLER M., BOLKER B., WALKER S., Fitting Linear Mixed-Effects Models Using lme4, J Stat Soft, 2015, 67(1).

[23] LAKENS D., Calculating and Reporting Effect Sizes to Facilitate Cumulative Science: A Practical Primer for t-Tests and ANOVAs, Front Psychol, 2013, 4:863.

[24] CUMMING G., The New Statistics: Why and How, Psychol Sci, 2014, 25(1):7-29.

[25] BENJAMINI Y., HOCHBERG Y., Controlling the False Discovery Rate: A Practical and Powerful Approach to Multiple Testing, Journal of the Royal Statistical Society Series B: Statistical Methodology, 1995, 57(1):289-300.

[26] WORLD MEDICAL ASSOCIATION, Declaration of Helsinki: Ethical Principles for Medical Research Involving Human Participants, World Medical Association, 2024.